Modeling and Analysis of IEEE 802.11ax OFDMA-based Random Access

Yang Hang, Der-Jiunn Deng, *Member, IEEE,* and Kwang-Cheng Chen, *Fellow, IEEE*

***Abstract*—With the progressive increase of dense WiFi networks deployment, IEEE 802.11ax, the task group aimed at High Efficiency WLAN (HEW) in dense scenario, makes revolutionary modifications on both MAC and PHY layer. Especially one feature on MAC layer is OFDMA-Based Random Access (OBRA) mechanism. In this paper, we develop a bi-dimensional Markov process to model of the OBRA and derive a closed-form expression of system efficiency and access delay. Our simulation results verify the accuracy of the model. Finally, the effects of system parameters, including the number of resource units (RUs) for random access, initial and maximum contention window, are evaluated.**

***Index Terms*—OFDMA-based Random Access, Multi-User PHY, OFDMA, 802.11ax, High Efficiency WLAN**

I. Introduction

During last decade, IEEE 802.11 has achieved a great success with enormous WiFi networks deployed for its high throughput and relative simplicity of implementation. According to Cisco Visual Network index [1], the global mobile traffic will experience an eightfold increase within 2015-2020, reaching 30.6 EB per month by 2020. Therefore, the *dense scenarios*, where there are plenty of stations (STAs) associating with one access point (AP) or multiple basic service sets (BSSs) in a limited area, is becoming a common scenario.

Previous IEEE 802.11 amendments made fewer improvement on MAC layer compared with that on PHY layer. A series of standards (802.11b/g/n/ac) have evolved to respond to the increasing WLAN demand, mainly by means of raising data rate on the physical layer (PHY) from 2 Mbps to 7 Gbps [2]. However, user experience of WiFi networks does not improve enough with the data rate, especially in the dense scenario. That is because few enhancement has been made to improve MAC efficiency. The MAC is always based on distributed coordination function (DCF) in legacy 802.11, which is a random access protocol on a Single-User (SU) PHY.

MAC efficiency mainly degrades with two causes, the overhead of control signaling and packet collisions. Much effort has been conducted in legacy 802.11 to reduce the overhead of control signaling, such as Reduced Inter-Frame Spacing (RIFS), frame aggregation, etc [2]. However, in the dense scenario, collision is becoming the major component of bandwidth waste. The collision comes inherently from instability of DCF [3]. In addition, an unfair queueing problem worsens the instability of DCF.

The unfair queueing problem results from both DCF and star topology of BSS. When the WiFi network is seen with queueing model, each STA and AP are modeled as an individual queue, and the shared channel as the server. Since the BSS operates in a star topology, AP as the coordinator and n STAs nearby, all STAs download or upload data from or to AP, which is referred to as down-link (DL) traffic and up-link (UL) traffic respectively. On the other hand, each STA and AP have the same chance to access the channel. Thus the AP shares the DL traffic loading, which accounts for more than $1/2$ of total traffic, while it only has chance of $1/(n+1)$ to access channel. The queue model of WiFi network is, therefore, an unfair queueing between DL and UL transmissions.

Study group 802.11ax, aimed at HEW in the dense scenarios, thus modifies the MAC thoroughly by substituting DCF with centralized control. On the PHY layer, OFDMA is the first time adopted by 802.11 to implement both the DL and UL Multi-User (MU) channel, which means a STA could communicate with multiple STAs simultaneously. On MAC layer, the AP is supposed to schedule both DL and UL transmissions, which means AP does not need to contend with STAs. As a result, instability of DCF should be mitigated and the unfair queueing problem does not exist anymore. Moreover, an OFDMA-based random access (OBRA) is proposed in 802.11ax as random access is highly efficient to deliver short frames, like bandwidth request. The OBRA mechanism proposes a three-way handshake procedure to implement random access. AP initiates the OBRA by transmitting an announce frame at first. STAs receiving the the announcement then contends with Aloha and binary exponential backoff mechanism. AP finally responds with ACK confirming which STAs contend successfully. Details of the mechanism will be illustrated in Section II.

[4] [5] [3] OBRA has been adopted by cellular networks to perform initial association to the network and to request transmission resource. In the literature, [6] [7] devoted to multi-channel slotted Aloha systems, [6] designed for satellite communication. In [7], reservation is considered. In recent years, related works have proposed some models to derive the throughput [8] [9] [10], the collision probability [11] [12], and the access delay [8] [11] [12]. [8] gives a closed-form expression of throughput for OFDMA system. [9] proposes a stabilized multi-channel slotted Aloha by pseudo-Bayesian algorithm. And [10] designs a 1-persistent type retransmission that avoids exponential backoff to achieve a fast access. Some other works [8] [12] [11] compare performance of two kinds of backoff mechanism, binary exponential backoff and uniform backoff, which are implemented by IEEE 802.16 and 3GPP LTE respectively. Especially, [14] specifies a model estimating transient behavior of OFDMA system with busty traffic. On

the other hand, it is the first time for 802.11 to adopt the MU-OFDMA in 802.11ax. Almost all previous works [15] [5] etc. about 802.11 MAC efficiency focused on CSMA/CA on SU PHY. One of few works [16] generalizes CSMA/CA to OFDMA system for 802.11.

In this paper, we use a Markov chain model to simply and accurately depict the steady state behavior of the OBRA mechanism. In [5], Markov chain model has been demonstrated to model DCF precisely. Though the OBRA differs much from DCF, including SU channel to MU channel, distributed MAC scheme to centralized MAC scheme, and carrier sense to Aloha, the Markov chain model still works well by some modifications adapting to these differences. And thereby, we are able to evaluate the system efficiency, access delay and effects of important system parameters.

The paper is organized as follows. Some necessary features of 802.11ax are illustrated in Section II, including MU-OFDMA and OFDMA-based random access procedure. Section III contains the system model and performance analysis. Then Section IV shows simulation results, along with analysis results to validate the model. In Section V, additional considerations on optimal performance are carried out and the effects of some important system parameters are evaluated. Conclusion remark is finally given in Section VI.

II. Preliminary

Some necessary features of 802.11ax to better understand the OBRA mechanism are illustrated in this section. First, MU-OFDMA is firstly adopted by 802.11 to implement MU DL and MU UL. To support MU UL, study group 802.11ax proposes TF-based UL procedure, which means UL transmission could be scheduled by AP, shifting distributed coordination to centralized control. Then OFDMA-based random access (OBRA) is illustrated in the following subsection. For more features of 802.11ax, refer to [17] [18].

A. MU-OFDMA

OFDM has been proposed as one of the prime schemes for MU communications. In such OFDM-based systems, the total bandwidth is divided into multiple sub-channels so that multiple access can be accommodated in an OFDMA. Though MU PHY has been implemented in 802.11n and 802.11ac with MU-MIMO, only MU DL transmission is realized. MU-OFDMA implements both MU DL and MU UL. Especially for MU UL transmission, which is more difficult to implement, trigger-based MU UL is thus proposed.

With MU PHY, the original SU 20 MHz channel could be specified more fine-grained and be also aggregated to a wider channel to meet various bandwidth demands. The resource unit (RU), which can be accessed by one STA, is specified as Table I. For example, the smallest RU is 26-tone, with which a 20 MHz could be separated into 9 subchannels. Also multiple 20 MHz channels can be aggregated to improve system throughput, which is referred to as *Channel Bonding*. It is worth mentioning that every transmission of MU should end at the same time. That means padding is required for shorter packets.

TABLE I: Maximum number of RUs for each channel width

RU type	CBW20	CBW40	CBW80	CBW80+80 and CBW160
26-tone RU	9	18	37	74
52-tone RU	4	8	16	32
106-tone RU	2	4	8	16
242-tone RU	1	2	4	8
484-tone RU	N/A	1	2	4
996-tone RU	N/A	N/A	1	2
2×996 tone RU	N/A	N/A	N/A	1

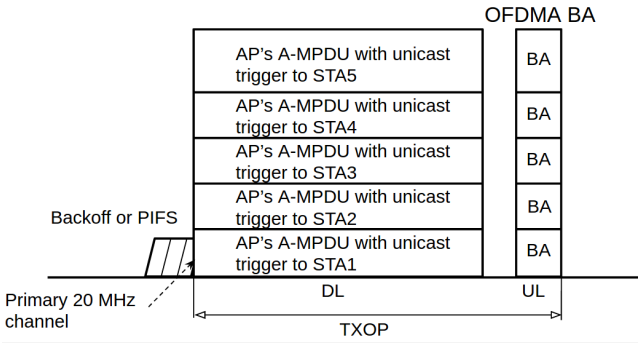

Fig. 1: MU DL of 802.11ax

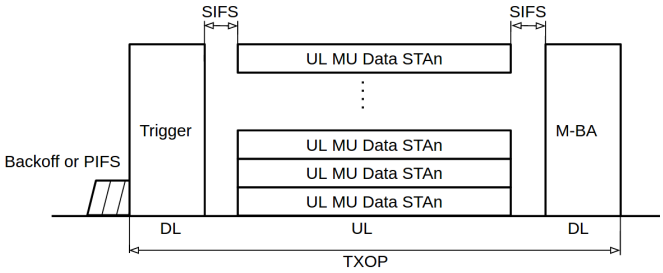

Fig. 2: Trigger-based MU UL of 802.11ax

In respect of MAC layer, first for MU DL transmission, AP transmits DL packets to multiple stations simultaneously as in Fig. 1. Secondly, MU UL transmission is more complicated because WiFi network is not a well-synchronized system. A trigger-based MU UL transmission is thus issued in Fig. 2. A brand new control frame, trigger frame (TF), is created to be transmitted by AP to initiate the UL transmission. STAs could not transmit UL packets until they receive a TF which allocates RU for the STA or specifies RUs for random access. Afterwards, AP responds with ACK frame. All the procedure form a three-way handshake UL transmission. The trigger frame format is in Fig. 3. Since the standard is in progress, some fields remain to be determined (TBD). In the field *User Info*, subfield *AID* represents the identification of STA and subfield *RU Allocation* represents the RU allocated to the STA. Especially, *AID* with value 0 means the RU is for random access.

B. OBRA

An example of TF-based MU UL transmission with OBRA, illustrated in Fig. 4, is divided into two steps, one as random access procedure and the other UL data transmission. The random access procedure, namely the OBRA, is initiated by

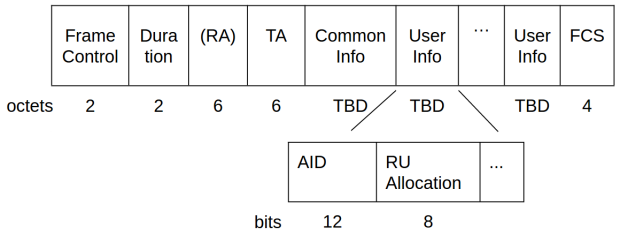

Fig. 3: Trigger Frame format

AP to collect traffic information named buffer state report (BSR) from stations. Thereby in the next step, the AP could allocate RUs to STAs by transmitting a TF containing RU allocation. Then the STAs, receiving the TF with resource allocation information, transmit UL data packets. And AP at last responds ACK. Therefore, TFs in the example have two variants, one for random access and the other for resource allocation. When traffic information is collected, the allocation is beyond the scope of this paper. Only step one is our interest.

Details of OBRA mechanism is as Fig. 5. To initialize a random access procedure, AP first transmits a TF announcing RUs for random access by setting the AID of the RUs to 0. Attempting STAs, whose buffers are not empty, maintain a backoff counter named OFDMA Backoff (OBO), which are randomly generated among range $[0, OCW]$. Then the OBO subtracts the value of M once receiving the TF, otherwise freezes, where M is calculated by sum the number of RUs whose AID equals 0. When the OBO reaches 0, the STA will randomly select a RU from those whose AIDs equal 0 to transmit a request after short inter-frame spacing (SIFS). After that, AP responds with a block-ACK indicating which STAs contend successfully. The period of the whole three-way handshaking is named a *stage*. A successful stage means at least one STA contend successfully to transmit a request in a stage. It is worth noting that the stage in this paper, which is specified from standard [17], is a concept of the time interval, not the backoff stage in other papers. To avoid confusion of the two meanings, backoff stage is replaced with *backoff level* in this paper. When STAs fail to contend, the OCW will be doubled until OCW reaches OCW_{max}, which means the backoff level increases one step once a failure until the highest level.

In terms of implementation, system parameters of the OBRA are configured dynamically by AP, including OCW_{min}, OCW_{max}, M, where OCW_{min}, OCW_{max} represent the minimum and the maximum contention window, and M as the number of RUs for random access. Two of critical parameters OCW_{min}, OCW_{max} are configured in Random Access Parameter Set (RAPS) element contained in beacon frame sent by AP. Check field *OCW Range* in RAPS element as in Fig. 6, $OCW_{min} = 2^{EOCW_{min}} - 1$, $OCW_{max} = 2^{EOCW_{max}} - 1$. M is obtained from TF by sum the number of RUs whose *AID* equal 0. To simplify following analysis, we issue another parameter m, *maximum backoff level*, so that $OCW_{max} = (OCW_{min} + 1) * 2^m - 1$. The configuration of system parameter is absolutely different from that of legacy 802.11, where all the parameters are predefined in each STA's hardware. OBRA is thus more flexible compared with DCF.

III. System Model

Markov chain model has been verified of its accuracy of depicting the steady state behavior of DCF based on the assumption that at each request transmission, and regardless of the number of retransmission suffered, each request frame collides with constant and independent probability p [5]. Although some differences exist between OBRA and DCF, following shows the accuracy of Markov chain model for OBRA mechanism.

The analysis is divided into two parts. First is the Markov chain model to estimate the packet transmission probability τ and conditional collision probability p. Secondly, we evaluate some metrics given τ, including the number of stations who succeed in contending in a stage n_s, self-defined system efficiency *eff*, and access delay of a STA D. Table II is a list of all parameters and notations.

TABLE II: Parameters and Notations Interpretation

Notations	Meaning
n	Number of stations
OCW_{min} (W_0)	Minimum OFDMA contention window
OCW_{max} (W_m)	Maximum OFDMA contention window
M	Number of RUs for random access
m	Maximum backoff level
p	Packet collision probability
τ	Station's transmission probability
n_s	Number of successful stations in a stage
D	Access delay, number of stages for a station to contend successfully

A. Packet Transmission Probability

Consider a single BSS with an AP and n of STAs under saturation condition, which means each station is an attempting station. Also, the ideal channel is assumed so that collision happens only if more than one station transmits at the same RU. Only UL BSR transmission (bandwidth request) is concerned, while DL transmission and UL data transmission are ignored here.

To model OBRA with the discrete-time Markov chain model, the concept of time is supposed to be adapted. In DCF, time unit of the model corresponds with slot, while in OBRA time unit of the model is stage, a three-way handshake. Thus the delay will be measured in the number of stages.

Similar to Bianchi's work, let $\{s(t), b(t)\}$ be the bi-dimension process, where $s(t)$ denotes the backoff level $(0, \cdots, m)$, and $b(t)$ denotes backoff counter $(0, \cdots, W_i)$. With the discrete and integer time scale, t and $t+1$ corresponds to beginnings of two consecutive stages. $\{b(t)\}$ is not a Markov process because the state of the current stage depends on the history of transmission instead of only the previous stage. The bi-dimensional process $\{s(t), b(t)\}$ is a Markov chain. The key assumption is still necessary that at each request transmission, and regardless of the number of retransmission suffered, each request frame collides with constant and independent probability p. With the independence assumption, p will be a constant. The Markov chain is able to be conducted as in Fig. 7.

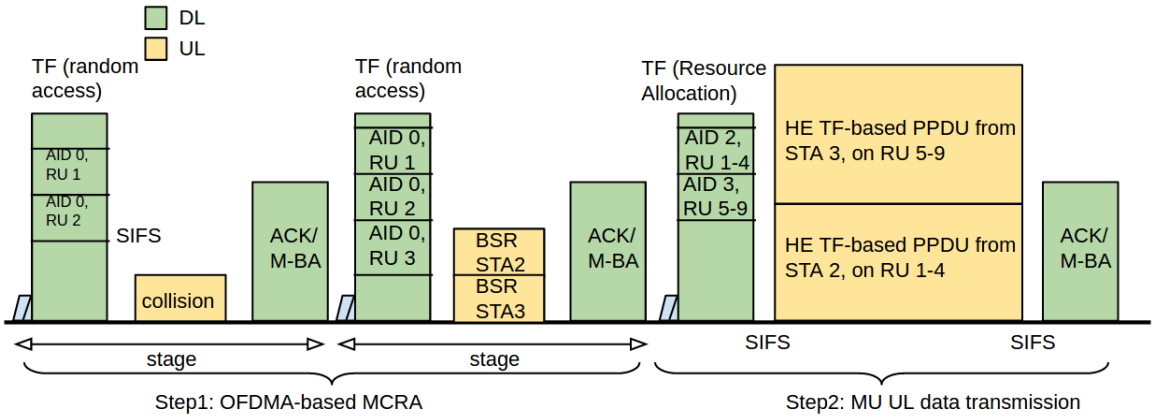

Fig. 4: An example of Trigger-based MU UL transmission with OBRA

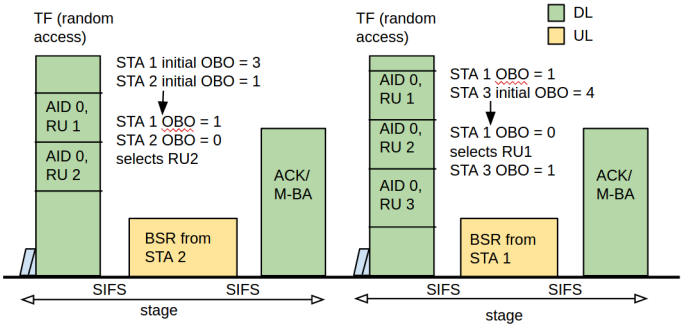

Fig. 5: Illustration of OBRA

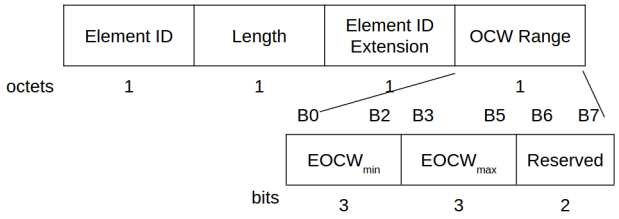

Fig. 6: Random Access Parameter Set (RAPS) Element

Another important difference between the two Markov chain models of OBRA and DCF, is clarified here. Since the station of DCF senses the carrier before transmitting, it will freeze its backoff counter and stay at the state if channel is sensed busy. However in the OBRA, because the time unit, a stage, contains a period for exactly a packet transmission, stations certainly subtract M from the OBO only if they receive a TF for random access. Stations of the OBRA thus stay in one state for a period of exactly single stage.

Some modifications are mentioned here to adapt to differences between OBRA and DCF. First, in a row of states, as OBO subtracts the value of M rather than 1, stations transfer to states M-step ahead. Second, since states with $b(t) \leq M$ will decrease to 0 at the current state, which means stations could access RUs, we could merge these states into one state, denoted by $\{i, T\}$. T is an integer set of $[0, M]$.

Let's assume $P\{i_1, k_1 | i_0, k_0\} = P\{s(t+1) = i_1, b(t+1) = k_1 | s(t) = i_0, b(t) = k_0\}$. In this Markov Chain, the only non null one-step transition probabilities are

$$\begin{cases} P\{i,T|i,k\} = 1 & k \in [M+1, 2M] \quad i \in [0,m] \\ P\{i,k-M|i,k\} = 1 & k \in [2M+1, W_i] \quad i \in [0,m] \\ P\{0,k|i,T\} = \frac{1-p}{W_0+1} & k \in [M+1, W_0] \quad i \in [0,m] \\ P\{0,T|i,T\} = \frac{(1-p)(M+1)}{W_0+1} & \quad i \in [0,m] \\ P\{i,k|i-1,T\} = \frac{p}{W_i+1} & k \in [M+1, W_i] \quad i \in [1,m] \\ P\{i,T|i-1,T\} = \frac{p(M+1)}{W_i+1} & \quad i \in [1,m] \\ P\{m,k|m,T\} = \frac{p}{W_m+1} & k \in [M+1, W_m] \\ P\{m,k|m,T\} = \frac{p(M+1)}{W_m+1} & \end{cases} \tag{1}$$

The first and second equations in (1) accounts for the fact that the backoff counter maintained by stations will subtract M, the number of RUs for random access. The third and fourth equations represent that after a successful contention, stations will reset the contention window size to initial window size and uniformly generate a backoff value among $[0, W_0]$, since T is an integer set $[0, M]$, the transition probability to states $\{i, T\}$ is $M+1$ times of that to states $\{i, k\}$. For the fifth and sixth equations, they represent when a failure contention occurs, the contention window size will be doubled, $W_i = 2W_{i-1}+1$. The last two equations are the case of failure at the maximum backoff level. We assume no packets are discarded, repeating retransmitting until success.

Let $b_{i,k} = \lim_{t\to\infty} P\{s(t) = i, b(t) = k\},\ i \in [0, m],\ k \in [0, W_i]$, be the stationary distribution of the Markov chain. Then we show how to obtain transmission probability τ and conditional collision probability p. First, for states with $b(t) = T$, in which stations will transmit requests or BSRs in current stage,

$$\begin{aligned} b_{i-1,T} \cdot p = b_{i,T} \to b_{i,T} = p^i b_{0,T}, \quad 0 \leq i < m \\ b_{m-1,T} \cdot p = (1-p) b_{m,T} \to b_{m,T} = \frac{p^m}{1-p} b_{0,T}. \end{aligned} \tag{2}$$

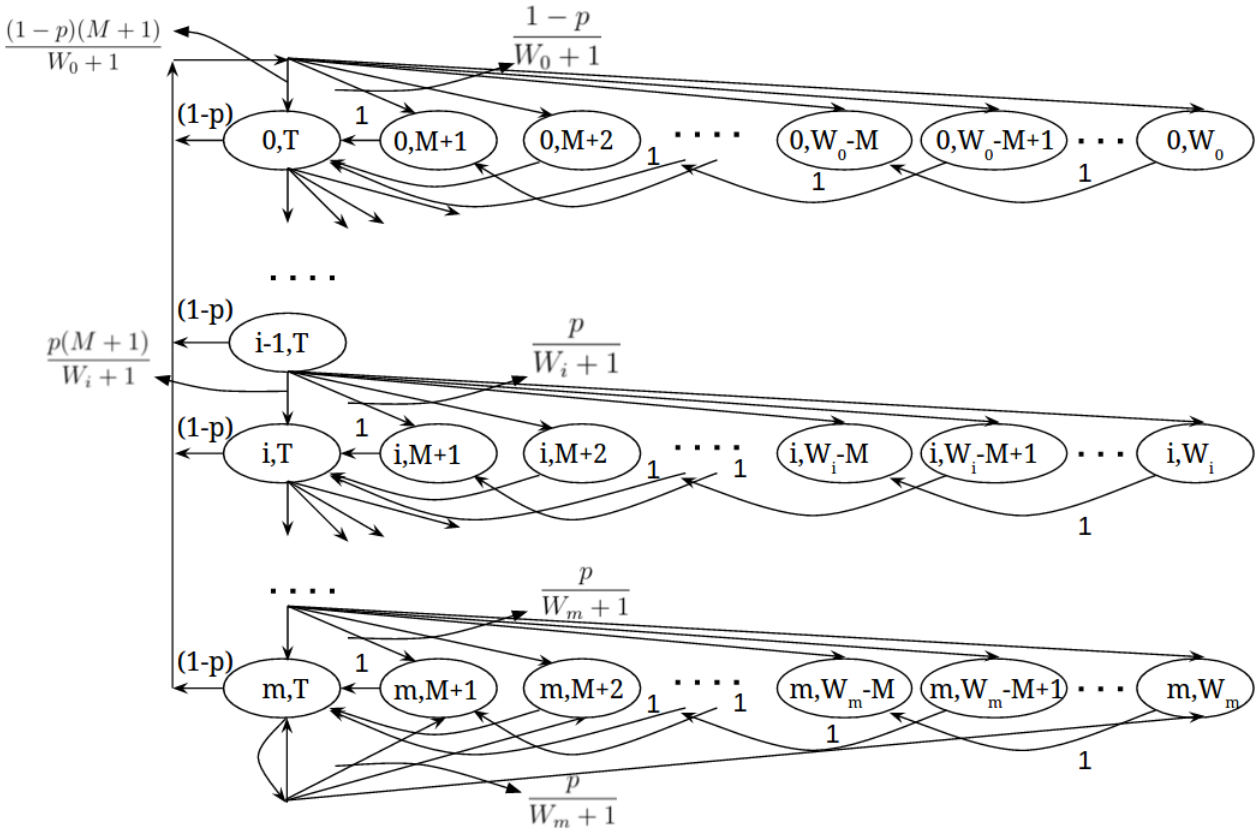

Fig. 7: Markov Chain model for the backoff window size

$$\begin{cases} \sum_{k=M+1}^{W_0} b_{0,k} = \frac{b_{0,T}}{W_0+1}\left(-\frac{M}{2}\left\lfloor\frac{W_0}{M}\right\rfloor^2 + \left(W_0 - \frac{M}{2}\right)\left\lfloor\frac{W_0}{M}\right\rfloor\right) \\ \sum_{i=1}^{m-1}\sum_{k=M+1}^{W_i} b_{i,k} = \frac{b_{0,T}}{W_0+1}\left(\frac{p}{2}\right)^i\left(-\frac{M}{2}\left\lfloor\frac{W_i}{M}\right\rfloor^2 + \left(W_i - \frac{M}{2}\right)\left\lfloor\frac{W_i}{M}\right\rfloor\right) \\ \sum_{k=M+1}^{W_m} b_{m,k} = \frac{b_{0,T}}{W_0+1}\frac{(\frac{p}{2})^m}{1-p}\left(-\frac{M}{2}\left\lfloor\frac{W_m}{M}\right\rfloor^2 + \left(W_m - \frac{M}{2}\right)\left\lfloor\frac{W_m}{M}\right\rfloor\right) \end{cases} \tag{4}$$

Then, other states are expressed with states where $b(t) = T$:

$$b_{i,k} = \begin{cases} (\lfloor\frac{W_0-k}{M}\rfloor+1)\frac{(1-p)}{W_0+1}\sum_{i=0}^{m} b_{i,T}, \ M+1 \le k \le W_0, \ i=0 \\ (\lfloor\frac{W_i-k}{M}\rfloor+1)\frac{p}{W_i+1}b_{i-1,T}, \ M+1 \le k \le W_i, \ 0<i<m \\ (\lfloor\frac{W_m-k}{M}\rfloor+1)\frac{p}{W_m+1}(b_{m-1,T}+b_{m,T}), \\ \qquad\qquad M+1 \le k \le W_m, \quad i=m \end{cases} \tag{3}$$

From (2), $\sum_{i=0}^{m} b_{i,T} = \frac{b_{0,T}}{1-p}$ is obtained; whereby (3) could be summed respectively to get (4).

Each subequation in (4) has the same term: $-\frac{M}{2}\left\lfloor\frac{W_i}{M}\right\rfloor^2 + \left(W_i - \frac{M}{2}\right)\left\lfloor\frac{W_i}{M}\right\rfloor$. To simplify the expression, let $X_i = -\frac{M}{2}\left\lfloor\frac{W_i}{M}\right\rfloor^2 + \left(W_i - \frac{M}{2}\right)\left\lfloor\frac{W_i}{M}\right\rfloor$. Then, sum the steady state probability of all states to get (6).

whereby a closed-form expression of τ, the probability of a station transmitting a request at a stage, is derived.

$$\tau = \sum_{i=0}^{m} b_{i,T} = \frac{b_{0,T}}{1-p} = \frac{W_0+1}{W_0+1+(1-p)X_0+(1-p)\sum_{i=1}^{m-1} X_i\left(\frac{p}{2}\right)^i + X_m\left(\frac{p}{2}\right)^m} \tag{7}$$

For $m = 0, M = 1$ which is SU PHY with a fixed contention window, check (5), the terms containing $X_i, i > 0$ will disappear, and $b_{0,T}/(1-p)$ degrades to $b_{0,T}$. As a result, (6) degrades to

$$1 = b_{0,T}\left(\frac{W_0+1+X_0}{W_0+1}\right). \tag{8}$$

Thereby,

$$\tau = b_{0,T} = \frac{W_0+1}{W_0+1+X_0} = \frac{2(W_0+1)}{W_0^2+W_0+2}, \tag{9}$$

$$1 = \sum_{i=0}^{m}\sum_{k=0}^{W_i} b_{i,k} = \frac{b_{0,T}}{W_0+1}\left(X_0 + \sum_{i=1}^{m-1} X_i \left(\frac{p}{2}\right)^i + X_m \frac{\left(\frac{p}{2}\right)^m}{1-p}\right) + \frac{b_{0,T}}{1-p} \tag{5}$$

$$= b_{0,T}\left(\frac{(1-p)X_0 + (1-p)\sum_{i=1}^{m-1} X_i \left(\frac{p}{2}\right)^i + X_m \left(\frac{p}{2}\right)^m + W_0 + 1}{(W_0+1)(1-p)}\right), \tag{6}$$

which is different from that of CSMA/CA with constant window size [19], where $\tau = \frac{2}{W_0+1}$. That is because stations of CSMA/CA freezes backoff counter when sensing busy channel while no such freeze mechanism of backoff counter exists in OBRA.

On the other hand, conditional collision probability p has another relation with the probability τ. With ideal channel assumption that the collision happens only if at least one of other stations select the same RU, we have

$$p = 1 - \left(1 - \frac{\tau}{M}\right)^{n-1}. \tag{10}$$

Rewrite (10) as $\tau^\star = \left(1 - (1-p)^{\frac{1}{n-1}}\right) M$. To obtain probability τ and p, we need to find solutions to a group of the two equations 7 and 10. $\tau^\star(p)$ is a monotonically increasing function. Though $\tau(p)$ is hard to determine the monotonicity from the expression of equation 7 with respect to p, the function 7 is estimated monotonically decreasing by numerical method. Also, $\tau(0) = \frac{W_0+1}{W_0+1+X_0} > \tau^\star(0) = 0$. And $\tau(1) < \tau^\star(1) = M$. Therefore, the only solution could be found by numerical method.

B. Random Access Efficiency

With the transmission probability τ, performance of OBRA mechanism could be easily evaluated. First, the expected number of stations who contend successfully at a stage, denoted by $E[n_s]$. Extending n_s, a system efficiency is defined as another important metric. Also, the access delay denoted by D, referred to as number of stages required for a station to contend successfully, could be derived.

1) n_s and System Efficiency: What we are concerned about is that how many stations contend successfully at a stage. Given τ and p, the probability that a station contend successfully in a stage is firstly derived: $P_{s\_station} = \tau(1-p)$. Then, with (10), $E[n_s]$ is easily expressed as follows.

$$\begin{aligned} E[n_s] &= nP_{s\_station} \\ &= n\tau(1-p) \\ &= n\tau(1-\frac{\tau}{M})^{n-1} \end{aligned} \tag{11}$$

Furthermore, normalizing n_s, *system efficiency* here is defined as the ratio of the number of successful contending stations in a stage to the number of RUs for random access in a stage.

$$\begin{aligned} \textit{eff}\ (\tau) &= \frac{E[n_s]}{M} \\ &= \frac{n\tau(1-\frac{\tau}{M})^{n-1}}{M} \end{aligned} \tag{12}$$

2) Access Delay: D represents the number of stages required for a station to contend successfully in a stage. Because of saturation assumption, a new request arrives once one previous request is transmitted successfully. Thus queueing waiting time is not considered here. In this way, the access delay D follows the geometric distribution with parameter $P_{s\_station}$, which is obtained just now. Then the expected value of access delay of request frame, $E[D]$, is

$$E[D] = \frac{1}{\tau(1-\frac{\tau}{M})^{n-1}}. \tag{13}$$

IV. Model Validation

The same with scenario for analysis, only OBRA mechanism, i.e., Fig. 5, is concerned. Simulation runs with three-way handshake stage by stage. We run simulations for 1,000,000 stages with a variety of parameter sets $\{M, OCW_{min}, OCW_{max}\}$ and collects the information of the two variables, the number of successful attempt STAs n_s and expected access delay D. The values of results from both analysis and simulation are given in Fig. 8 and Table III. The results show that the Markov model precisely predicts the steady state behavior of the OBRA mechanism.

TABLE III: Analysis versus simulation: n_s and access delay with $m = 3, M = 9, OCW_{min} = 15$

n_s	analysis	simulation
$n = 1$	0.72727	0.72728
$n = 5$	2.23001	2.22335
$n = 10$	2.88954	2.88546
$n = 20$	3.29798	3.29857
delay	analysis	simulation
$n = 1$	1.37500	1.37499
$n = 5$	2.24214	2.24886
$n = 10$	3.46075	3.46565
$n = 20$	6.06432	6.06323

V. Performance Evaluation

With above analysis, we could conveniently evaluate performance, including system efficiency and access delay, and the effects of system parameters. Since the model acts quite precisely, model analysis is solicited to evaluate the performance later.

A. Maximum System Efficiency and Minimum Access Delay

With the system efficiency given in (12), take the derivative with respect to τ, and find the extreme point, $\tau^\star = M/n$.

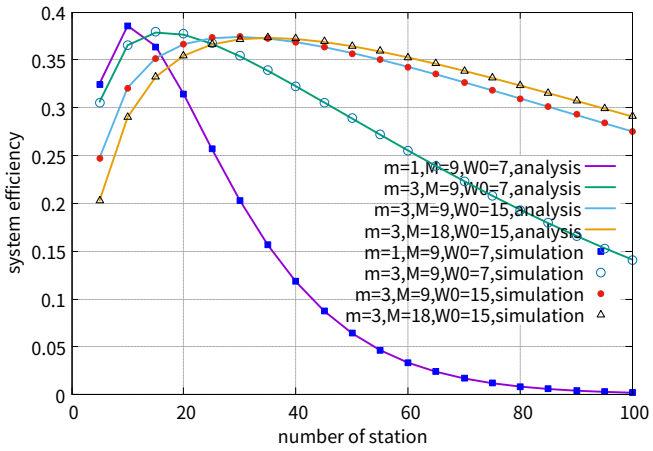

Fig. 8: System efficiency: Analysis versus Simulation

Since $\tau \in [0,1]$, $\tau^\star = min\{1, M/n\}$. In the dense scenario, i.e., n is large, then $\tau^\star = M/n$. The system efficiency thus is

$$\textit{eff}\ (\tau^\star) = (1 - \frac{1}{n})^{n-1} \tag{14}$$

Then the maximum n_s is

$$E[n_s]^\star = M \cdot \textit{eff}\ (\tau^\star) = M(1 - \frac{1}{n})^{n-1}. \tag{15}$$

The limit of system efficiency, based on infinite n, is

$$\lim_{n\to\infty} \textit{eff}\ (\tau^\star) = \lim_{n\to\infty} (1 - \frac{1}{n})^{n-1} = \frac{1}{e} \tag{16}$$

which is the same with efficiency of SU slotted Aloha [20].

With the delay analysis given in (13), take the derivative with respect to τ, and find the extreme point, $\tau^\star = M/n$. Also, $\tau^\star = min\{1, M/n\}$. When $n \geq M$, the minimum access delay is

$$D(\tau^\star) = \frac{n}{M(1 - \frac{1}{n})^{n-1}}. \tag{17}$$

From above analysis, we find that the maximum system efficiency and minimum access delay are both obtained by the $\tau^\star = min\{1, M/n\}$. What's more, optimal system efficiency is independent with M, while M affects access delay. The larger M is, the shorter the access delay will be. It indicates that when AP allocates RUs for random access, the AP could allocate as many as possible.

Since τ and p are obtained by solving group equations (7) and (10), it's hard to give a closed-form expression of τ only depending on system parameters, M, W_0, m and n. The only way to catch the insights of the OBRA is to tune the system parameters $\{M, W_0, W_m\}$ one by one.

B. RUs for Random Access M

(14) has indicated that M, has nothing to do with optimal system efficiency. However, n_s and D are proportional and inversely proportional to M respectively according to (15) and (17). Following analysis results validate the statement.

In Fig. 9a, the maximum system efficiency from various cases are almost the same, approaching $1/e$. The only difference is "where" the optimal point locates. Practically, the

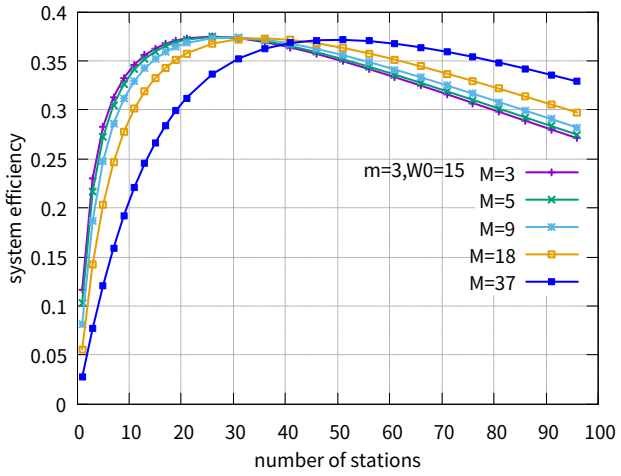

(a) System efficiency versus number of stations

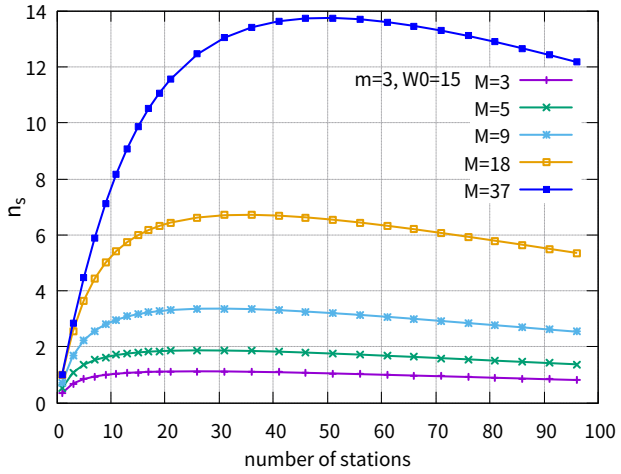

(b) Number of successful stations in a single stage versus number of stations

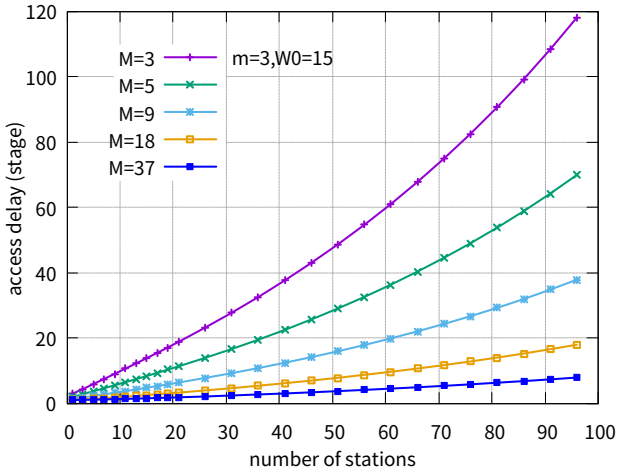

(c) Access delay versus number of stations

Fig. 9: Configure M

other two metrics, n_s and D, are closely related to M. Fig. 9b shows that larger M results more stations contend successfully in a stage. Moreover, Fig. 9c shows that larger M markedly decrease the access delay. Above all, when AP

allocates RUs for random access, AP should allocate as many RUs as possible.

C. OCW_{min}, OCW_{max}

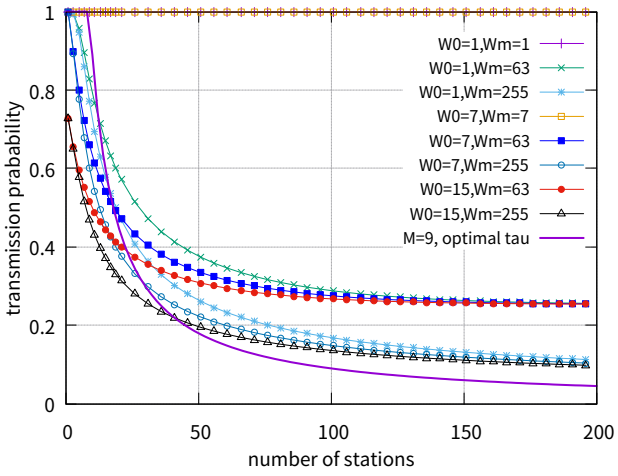

(a) Case 1, given $M = 9$

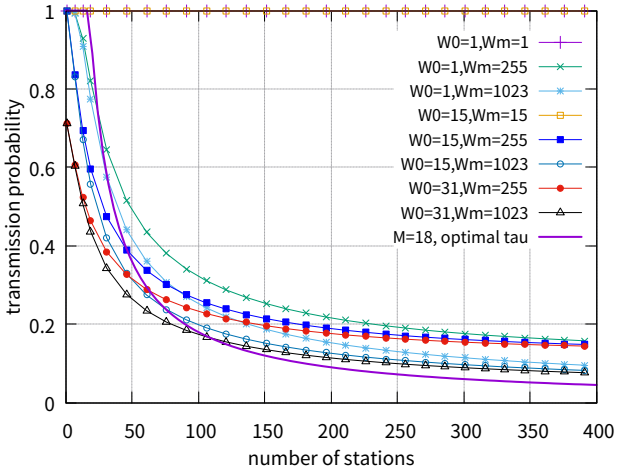

(b) Case 2, given $M = 18$

Fig. 10: Transmission probability versus number of stations

Fig. 10 shows case 1 ($M = 9$) and case 2 ($M = 18$), so that the rules we get are more convinced. In the figure, the purple line without point depicts the $\tau^\star$ that $\tau^\star = min\{1, M/n\}$. With above analysis and effects of M, we tune remaining parameters OCW_{min}, OCW_{max} so that τ approaches the optimal line. To see the trend of the line clearly, larger n is configured so that some rules could be obtained as follows.

First, the OCW_{min} or W_0, determines τ with small n. The larger W_0 is, the lower τ is at $n = 1$. That's why cases in Fig. 10 have two different start points.

Secondly, $m = 0$ results in constant τ, which is consistent with (9) that τ does not depend on n. A special case, $W_0 < M$ for scenario $n \leq M$, results in constant τ equals to 1 regardless of n. It perfectly matches $\tau^\star$ at $n \leq M$ as $\tau^\star = 1$ for the scenario $n \leq M$. Thus, if given $n \leq M$, the optimal configuration will be $OCW_{max} = OCW_{min} < M$.

Thirdly, performance of the dense scenario strongly depends on OCW_{max}. It determines the limit of the τ, i.e., where the line of τ will converge. And both the two figures in Fig. 10 correspond with the above statement. And larger W_m causes lower τ, which is closer to $\tau^\star$ when n is large.

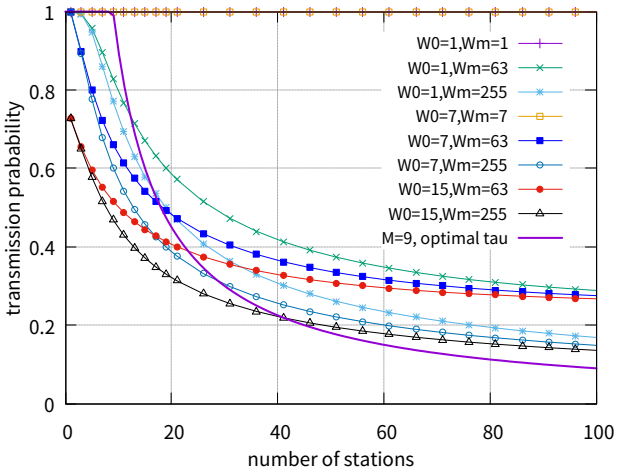

(a) Case 1, given $M = 9$

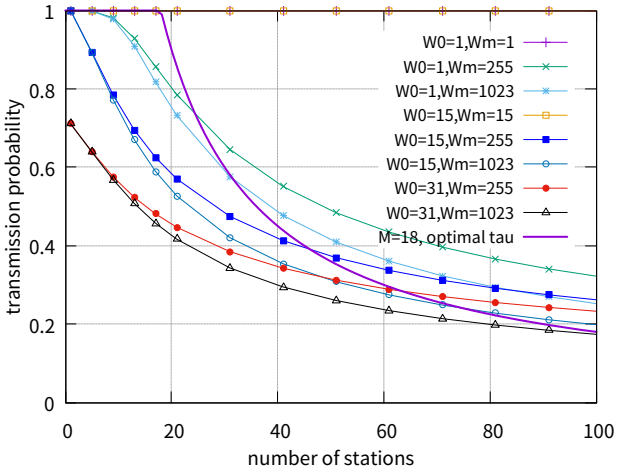

(b) Case 2, given $M = 18$

Fig. 11: Details of transmission probability versus number of stations when $n \leq 100$

Then, two subfigures as in Fig. 11 are generated from Fig. 10 with n ranges from $[0, 100]$ to observe practical scenarios more clearly. Another observation whereby is that when $W_0 = 1$, line of τ will have a flat start, which happens to match better with $\tau^\star$ at $n \leq M$.

All above observations are summed up that W_0 has significant influence on scenario of $n \leq M$, while W_m counts when n is large, namely the dense scenario. In the next two subsections, the system efficiency and access delay under different parameter configurations are practically evaluated, whereby above observed effects of parameters could be conformed.

1) Configure OCW_{max}: With above rough rules, the effect of OCW_{max} is first evaluated by setting different OCW_{max} while fixing $OCW_{min} = 1$ and $M = 9$. In Fig. 12a, three cases which has the same OCW_{min} are selected to clearly

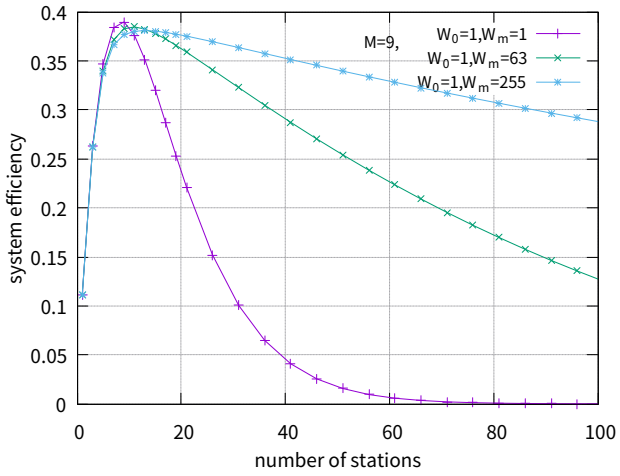

(a) System efficiency versus number of stations

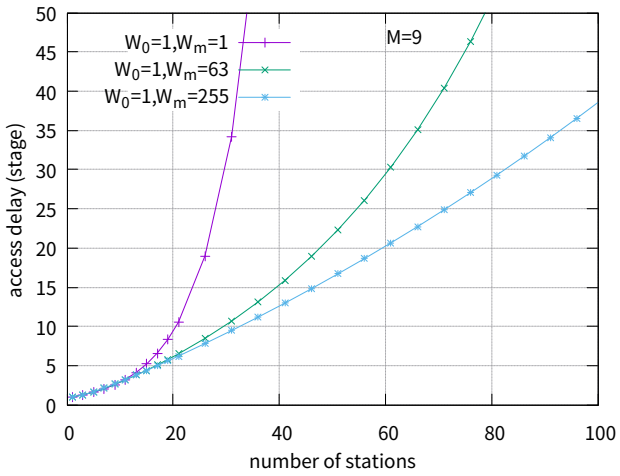

(b) Access delay versus number of stations

Fig. 12: Example of Configuring OCW_{max}, given $M = 9$

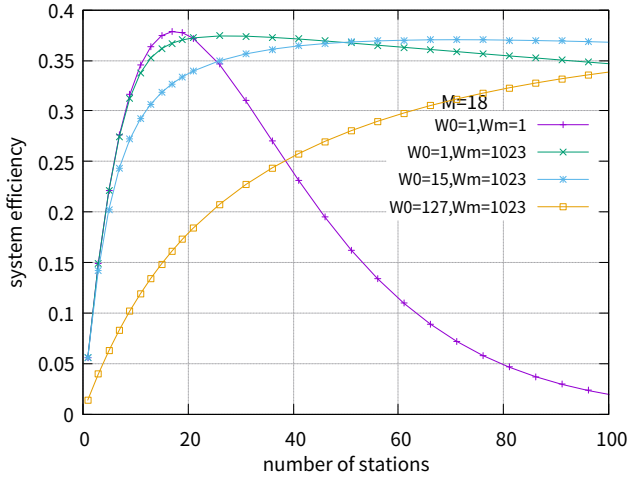

(a) System efficiency versus number of stations

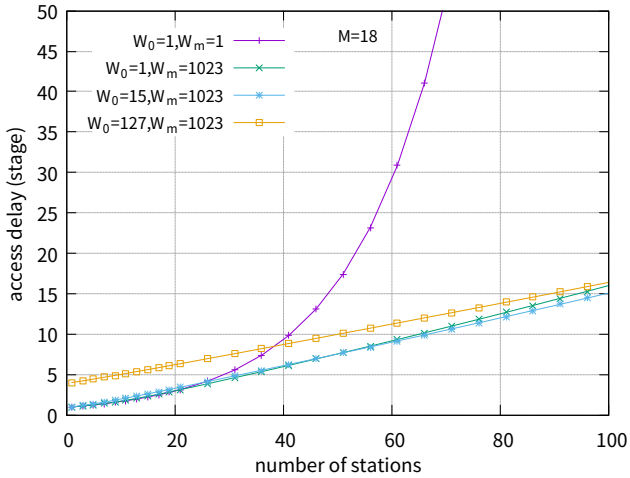

(b) Access delay versus number of stations

Fig. 13: Example of Configuring OCW_{min}, given $M = 18$

display the effect of OCW_{max} on system efficiency. From the figure, it is evident that larger OCW_{max} is much better for system efficiency when $n \geq M$. The result corresponds to the above rules obtained from the effect of parameters on τ. Additionally, larger OCW_{max} results in shorter access delay.

2) Configure OCW_{min}: To estimate the effect of OCW_{min}, the performance of different configurations of OCW_{min} while fixing large $OCW_{max} = 1023$, and $M = 18$. First, OCW_{min} determines the start of the probability τ, and it has a significant influence on the scenario of $n \leq M$. From Fig. 13a and 13b, we find larger $OCW_{min} = 127$ has lower system efficiency and larger access delay. Secondly, as stated in Section V-C that $W_0 = W_m \leq M$ is the perfect configuration in the scenario of $n \leq M$, it is validated in Fig. 13 that maximum system efficiency and minimum access delay are achieved with the configuration in the scenario of $n \leq M$. However, the configuration of small OCW_{min} and large OCW_{max} almost achieves as good performance as the perfect configuration.

To this end, all observed rules are listed as follows.

1 For M: the larger the better

2 For OCW_{min}, OCW_{max}:
- OCW_{min} counts when $n \leq M$. Smaller OCW_{min} is better.
- OCW_{max} counts when $n > M$. Larger OCW_{max} is better.

- Special case: for $n \leq M$
  $OCW_{max} = OCW_{min} < M$ is the optimal configuration.

VI. Conclusion

In this paper, we are the first to propose a Markov chain model conducting saturation analysis of the OBRA of 802.11ax. The simple Markov chain model is validated that it could accurately depict the steady state behavior of the OBRA. Thereby, closed-form expressions of system efficiency and access delay are derived. Finally, it is observed that performance strongly depends on the system parameters. Larger number of RUs or subchannels for random access results in more successful contending stations in a stage. The initial contention window has significant influence when only a few stations

exist, while maximum contention window counts in the dense scenario.

Different from DCF of legacy 802.11, the OBRA mechanism is more flexible, with system parameters dynamically configured. A real-time algorithm is required to configure the system parameters dynamically. This paper takes the first step to catch some insight from the steady state behavior of the OBRA mechanism. In the future, transient analysis is necessary to generate a configuration algorithm.

REFERENCES

[1] "Cisco Visual Networking Index:Forecast and Methodology, 2015-2020." [Online]. Available: http://www.cisco.com/c/en/us/solutions/collateral/service-provider/visual-networking-index-vni/complete-white-paper-c11-481360.pdf

[2] E. Perahia and R. Stacey, *Next Generation Wireless LANS: 802.11 n and 802.11 ac*. Cambridge university press, 2013.

[3] D. P. Bertsekas, R. G. Gallager, and P. Humblet, *Data networks*. Prentice-Hall International New Jersey, 1992, vol. 2.

[4] C.-H. Wei, R.-G. Cheng, and S.-L. Tsao, "Modeling and estimation of one-shot random access for finite-user multichannel slotted ALOHA systems," *IEEE Communications Letters*, vol. 16, no. 8, pp. 1196–1199, 2012.

[5] G. Bianchi, "Performance analysis of the IEEE 802.11 distributed coordination function," *IEEE Journal on selected areas in communications*, vol. 18, no. 3, pp. 535–547, 2000.

[6] H. Tan and H. Wang, "Performance of multiple parallel slotted Aloha channels," in *Proc. INFOCOM*, vol. 87, 1987, pp. 931–940.

[7] Z. Zhang and Y.-J. Liu, "Multichannel Aloha data networks for personal communications services (PCS)," pp. 21–25, 1992.

[8] P. Zhou, H. Hu, H. Wang, and H.-h. Chen, "An efficient random access scheme for OFDMA systems with implicit message transmission," *IEEE transactions on wireless communications*, vol. 7, no. 7, pp. 2790–2797, 2008.

[9] D. Shen and V. O. Li, "Performance analysis for a stabilized multichannel slotted ALOHA algorithm," in *Personal, Indoor and Mobile Radio Communications, 2003. PIMRC 2003. 14th IEEE Proceedings on*, vol. 1. IEEE, 2003, pp. 249–253.

[10] Y.-J. Choi, S. Park, and S. Bahk, "Multichannel random access in OFDMA wireless networks," *IEEE Journal on Selected Areas in Communications*, vol. 24, no. 3, pp. 603–613, 2006.

[11] S. Kim, J. Cha, S. Jung, C. Yoon, and K. Lim, "Performance evaluation of random access for M2M communication on IEEE 802.16 network," in *Advanced Communication Technology (ICACT), 2012 14th International Conference on*. IEEE, 2012, pp. 278–283.

[12] J.-B. Seo and V. C. Leung, "Design and analysis of backoff algorithms for random access channels in UMTS-LTE and IEEE 802.16 systems," *IEEE Transactions on Vehicular Technology*, vol. 60, no. 8, pp. 3975–3989, 2011.

[13] A. B. Behroozi-Toosi and R. R. Rao, "Delay upper bounds for a finite user random-access system with bursty arrivals," *IEEE transactions on communications*, vol. 40, no. 3, pp. 591–596, 1992.

[14] C.-H. Wei, G. Bianchi, and R.-G. Cheng, "Modeling and analysis of random access channels with bursty arrivals in OFDMA wireless networks," *IEEE Transactions on Wireless Communications*, vol. 14, no. 4, pp. 1940–1953, 2015.

[15] F. Calì, M. Conti, and E. Gregori, "Dynamic tuning of the IEEE 802.11 protocol to achieve a theoretical throughput limit," *IEEE/ACM Transactions on Networking (ToN)*, vol. 8, no. 6, pp. 785–799, 2000.

[16] H. Kwon, H. Seo, S. Kim, and B. G. Lee, "Generalized CSMA/CA for OFDMA systems: protocol design, throughput analysis, and implementation issues," *IEEE Transactions on Wireless Communications*, vol. 8, no. 8, pp. 4176–4187, August 2009.

[17] *Part 11: Wireless LAN Medium Access Control (MAC) and Physical Layer (PHY) Specifications, Amendment 6: Enhancements for High Efficiency WLAN*, IEEE Std. 802.11ax/Draft 1.0 Std., 2016.

[18] D.-J. Deng, S.-Y. Lien, J. Lee, and K.-C. Chen, "On Quality-of-Service Provisioning in IEEE 802.11 ax WLANs," *IEEE Access*.

[19] T.-S. Ho and K.-C. Chen, "Performance analysis of IEEE 802.11 CSMA/CA medium access control protocol," vol. 96, pp. 407–411, 1996.

[20] L. G. Roberts, "ALOHA packet system with and without slots and capture," *ACM SIGCOMM Computer Communication Review*, vol. 5, no. 2, pp. 28–42, 1975.

Yang Hang Biography text here.

Der-Jiunn Deng Biography text here.

Kwang-Cheng Chen Biography text here.